Machine Learning-Based Direction-of-Arrival Estimation

A Thesis Submitted

In Partial Fulfilment of the Requirements

for the course of

Undergraduate Research

by

Ishaan Reddy

(PRN:210200019)

To the

School of Computing and Data Science

Sai University

June 2024

CERTIFICATE

This is to certify that the work contained in the thesis entitled "**Machine Learning-Based Direction-of-Arrival Estimation**" by **Ishaan Reddy (PRN: 210200019)** has been carried out under my supervision.

Date: 08/07/2024

Dr. Ashok Chandrasekaran
Assistant Professor
School of Computing and Data Science
Sai University, Chennai

Abstract

This research addresses the challenge of Direction-of-Arrival (DoA) Estimation using a machine learning-based approach. The study introduces a single-channel approach that utilizes the quadrature-phase (QP) component of the space-time covariance matrix (STCM) as a feature vector for training machine learning models, thereby ensuring a unique mapping between feature and target variables. To validate this approach, radial basis function neural network (RBFNN) and support vector regression (SVR) are employed as benchmark models. Simulation results demonstrate that the proposed approach outperforms the existing approach in terms of reliability and accuracy, even under conditions of fewer array elements, data snapshots and low signal-to-noise ratio (SNR). Furthermore, the proposed approach enhances efficiency by reducing computational complexity during training and testing, leading to shorter execution times. However, the single channel approach still fails to address the issue of endfire prediction.

Therefore, a modified single-channel approach is proposed to resolve the endfire predictions that involves taking the phase of the elements of the space-time covariance matrix (STCM). This modified approach is validated using SVR, K-Nearest Neighbours (KNN) and Convolutional Neural Network (CNN) models. Simulation results suggest that the modified single-channel approach outperforms the existing approach in terms of reliability and accuracy, under various conditions that include lesser number of array elements, data snapshots and low signal-to-noise ratio (SNR) for endfire prediction. Additionally, it showcases superior estimation accuracy when trained with an increased angular spacing and under the influence of mutual coupling, all while exhibiting lesser execution time.

Acknowledgement

I would like to express my sincere gratitude to my supervisor, Professor Ashok Chandrasekaran for his invaluable time, guidance and support throughout the duration of my research. His academic rigour and passion in research motivated me to achieve a significant learning outcome. I am especially grateful for his patience in introducing and explaining the theories behind the problem statement.

Additionally, I would like to thank the faculty panel for attentively listening to my presentation and providing constructive feedback, which will enhance the quality of my future work.

Contents

List of Figures **vii**

List of Tables **viii**

1 Introduction **1**

1.1 Motivation 1

1.2 Research Objectives 2

1.3 Data Model 2

1.4 Existing Approach 3

2 Single Channel Approach **5**

2.1 Proposed Formulation 5

2.1.1 Training Setup 8

2.1.2 Testing Setup 8

2.2 Simulation Results and Analysis 8

2.2.1 Complexity Analysis 8

2.2.2 Estimation Reliability 10

2.2.3 Estimation Accuracy 11

2.2.4 Computation Complexity and Execution Time 12

3 Modified Single Channel Approach **14**

3.1 Proposed Formulation 14

3.2 Simulation Results and Analysis 15

3.2.1 Estimation Reliability 15

3.2.2 Estimation Accuracy 16
3.2.3 Execution time 20

4 Conclusion and Future Perspectives **22**

Appendix A **23**

Publications **25**

References **26**

List of Figures

1.1 Configuration of the data model 3
1.2 Process flow of the existing approach 4

2.1 Process flow of the single channel approach 7
2.2 Reliability comparison: (a)-(d) under $\sigma_n^2 = 0$, (e)-(h) under $\sigma_n^2 = 0.1$ 10
2.3 Accuracy comparison versus number of array elements 11
2.4 Accuracy comparison versus number of snapshots 11
2.5 Accuracy comparison versus SNR 12
2.6 Training complexity comparison versus number of array elements 12
2.7 Testing complexity comparison versus number of array elements 13

3.1 $\measuredangle(u_{p,q})$ versus theta 15
3.2 Process flow of the modified single channel approach 15
3.3 Reliability of endfire prediction comparison: (a)-(f) under $\sigma_n^2 = 0$, (g)-(l) under $\sigma_n^2 = 0.1$ 17
3.4 Accuracy of endfire prediction versus number of array elements 18
3.5 Accuracy of endfire prediction versus number of snapshots 18
3.6 Accuracy of endfire prediction versus SNR 19
3.7 Accuracy versus C_1 20

A.1 Training accuracy versus hyperparameters (Single Channel Approach) 23
A.2 Training accuracy versus hyperparameters (Modified Single Channel Approach) 24

List of Tables

2.1 Complexity comparison (Existing approach) 9
2.2 Complexity comparison (Proposed approach) 9
2.3 Execution time comparison 13

3.1 Training and testing accuracy comparison for $\Delta\theta = 5^\circ$ 19
3.2 Execution time comparison (Modified Single Channel Approach) 21

Chapter 1

Introduction

In sensor array and multichannel (SAM) research, direction-of-arrival (DoA) estimation is one of the cores and widely studied areas. Initial attempts to address the problem of DoA estimation are broadly categorized into classical methods, maximum likelihood (ML) methods, subspace-based methods, and integrated methods [4]. Within subspace-based methods, techniques such as multiple signal classification (MUSIC) and estimation of signal parameters via rotational invariance (ESPRIT) and its variants are considered benchmarks for evaluating advances in DoA estimation [5, 6]. Later, compressive sensing (CS) is widely studied for DoA estimation under sparsity and underdetermined framework [7, 8].

Machine learning (ML) has been extensively employed across various domains in signal processing, including the area of DoA estimation, which is no exception. In ML-based approaches, DoA estimation is treated as the approximation of a non-linear function, which maps the received array output to the DoA of the incoming target. This can be effectively accomplished through learning-based methods such as radial basis function neural network (RBFNN) [10–13], support vector regression (SVR) [14–17], k-nearest neighbours (KNN) [28] and convolutional neural networks (CNN) [26, 27].

1.1 Motivation

Traditionally, its applications have been mainly limited to the defence sector, such as radio detection and ranging (RADAR) and sound navigation and ranging (SONAR) [1, 2]. However,

today, it plays a crucial role in various applications, including ultrasound imaging, vehicular RADAR for autonomous driving, microphone array for human-machine interface (e.g., Amazon Echo, Audio Zooming), and multiple-input and multiple-output (MIMO) antenna arrays for Wi-Fi and mobile communication standards (IEEE 802.11n, IEEE 802.11ac, 5G, and beyond) [3].

With the increasing complexity and performance demands of these modern applications, traditional methods of DoA estimation face significant challenges. With a focus on reducing the computational complexity for DoA estimation, ML methods have been employed [9]. It enhances the accuracy, robustness, and efficiency of DoA estimation, thus addressing the limitations of conventional approaches and meeting the needs of advanced technological systems.

1.2 Research Objectives

(1) Proposing a single-channel approach to train machine learning (ML) models.

(2) Ensuring the uniqueness of the mapping between feature and target variables in the proposed approach, thereby enabling effective DoA estimation using ML feasible.

(3) Effectively improving the estimation reliability, estimation accuracy and reducing the computational complexity in the training and testing phases.

1.3 Data Model

Consider M far-field (plane wave) targets from direction angles $\Theta = \{\theta_m\}_{m=1}^{M}$ impinging on an Nelement uniform linear array (ULA) with a field-of-view (FOV) such that $\theta_m \in (-90^\circ, +90^\circ)$ as shown in Fig. 1.1. Then, the output of the ULA in the baseband, $\mathbf{x}(t) \in \mathbb{C}^{N\times 1}$ can be expressed as

$$\mathbf{x}(t) = \sum_{m=1}^{M} \mathbf{a}\left(\theta_m\right) s_m(t) + \mathbf{n}(t), t = 1, 2, \ldots, T \tag{1.1}$$

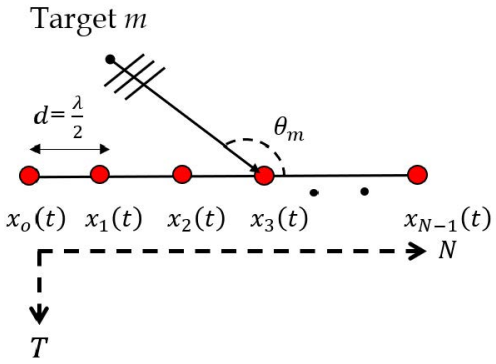

Figure 1.1: Configuration of the data model

where T represents the number of data snapshots. $\mathbf{a}(\theta_m) \in \mathbb{C}^{N\times 1}$ denotes the array directional vector associated with the m^{th} target direction angle $\theta_m \in \mathbb{R}^1$ is given by

$$\mathbf{a}(\theta_m) = [1e^{-jk\sin(\theta_m)} \cdots e^{-jk(M-1)\sin(\theta_m)}]^T \tag{1.2}$$

where $k = \frac{2\pi d}{\lambda}$, $d = \frac{\lambda}{2}$ is the inter-element spacing of the ULA, λ is the wavelength of the target signal. $s_m(t) \in \mathbb{C}^{M\times 1}$ denotes the signal amplitude of the m^{th} target. $\mathbf{n}(t) \in \mathbb{C}^{N\times 1}$ represents the additive white Gaussian noise with zero mean and covariance $\mathrm{E}\{\mathbf{n}(t)\mathbf{n}^H(t)\} = \sigma_n^2\mathbf{I}_N$, where σ_n^2 is the noise power and $\mathbf{I}_N$ denotes the $N \times N$ identity matrix [11].

1.4 Existing Approach

In both existing RBFNN and SVR-based formulations, the array space-time covariance matrix (STCM) mapped to its corresponding DoA of the incoming targets, is approximated using RBFNN and SVR respectively. The STCM is Hermitian symmetric, and its upper triangular region contains the necessary DoA information [11]. Therefore, its vectorized form is considered as an input feature to train the RBFNN and SVR models. However, the input features are complex-valued, and ML models cannot handle complex-valued data directly [18, 19]. To address this, the straightforward approach to make real-valued machine learning techniques applicable to complex-valued data is through the dual-channel formulation [20]. The underlying idea is to transform the complex-valued data into two uncorrelated real-valued ones. This approach ignores the correlation between the real and imaginary components of the complex-valued data, thus imposing limitations on the generalization capability and

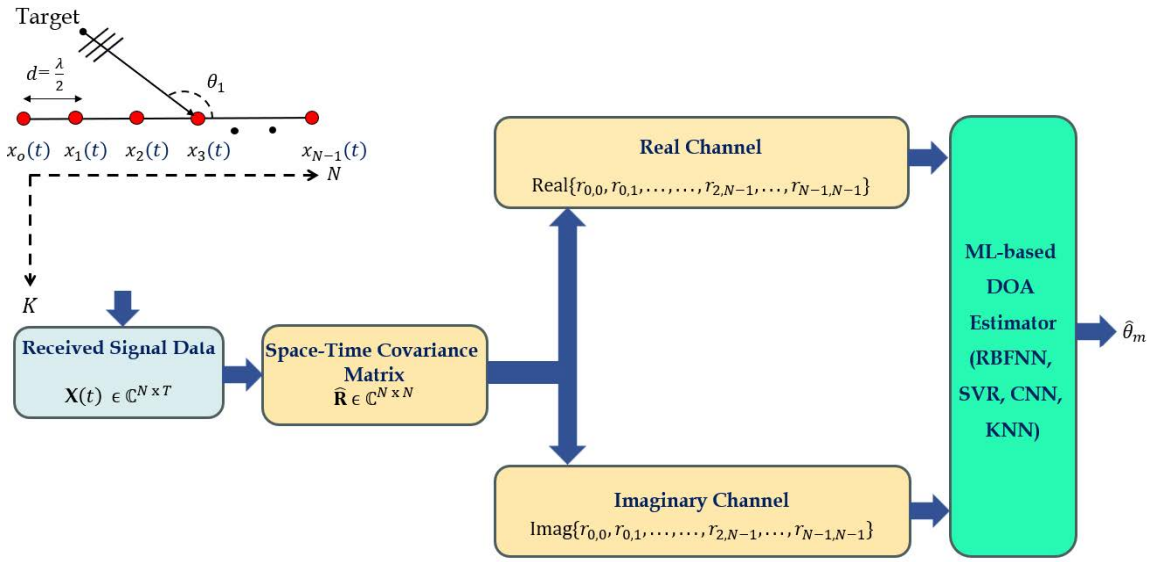

Figure 1.2: Process flow of the existing approach

robustness of the models and also effectively doubles the number of original feature vector values as observed in Fig. 1.2.

Chapter 2

Single Channel Approach

This section details the formulation of the proposed approach. Simulation results of the proposed approach and the existing approach are compared across various metrics such as estimation reliability, accuracy, computational complexity and execution time.

2.1 Proposed Formulation

The proposed approach aims to approximate the unknown mapping that relates the quadrature phase of the array STCM $\Im(\mathbf{R})$ to its corresponding DoA (θ) of the incoming targets. This mapping represented as $\widehat{F} : \Im(\mathbf{R}) \rightarrow \theta$, is achieved using ML models such as RBFNN and SVR receptively. The STCM is defined as follows

$$\mathbf{R} = \mathbf{E}\left\{\mathbf{x}(t)\mathbf{x}^H(t)\right\} \tag{2.1}$$

In practice, the STCM $\mathbf{R}$ is typically unknown and must be estimated from the received data $\mathbf{x}(t)$ [16]. The estimated STCM for T snapshots of data $\mathbf{x}(t)$ can be expressed as

$$\widehat{\mathbf{R}} = \frac{1}{T}\sum_{k=1}^{T}\mathbf{x}_k(t)\mathbf{x}_k^H(t) \in \mathbb{C}^{N\times N} \tag{2.2}$$

$$\widehat{\mathbf{R}} = \begin{pmatrix} r_{0,0} & r_{0,1} & \cdots & r_{0,N-1} \\ r_{1,0} & r_{1,1} & \cdots & r_{1,N-1} \\ \vdots & \vdots & \cdots & \vdots \\ r_{N-1,0} & \cdots & \cdots & r_{N-1,N-1} \end{pmatrix} \tag{2.3}$$

where $r_{p,q}$ represents the covariance between the p^{th} and q^{th} array element received data and it is given by

$$r_{p,q} = cov\left(x_p(t), x_q(t)\right); p, q \in \{0, 1, \ldots, N-1\} \tag{2.4}$$

where $cov(.)$ represents the covariance of (.). In $\widehat{\mathbf{R}}$, the diagonal elements correspond to the received power of each array element, while the off-diagonal elements represent the phase delays experienced by the target signals (plane wave) as it reaches each element in the array.

Upon simplifying the Equation (2.4), it follows

$$\begin{aligned} r_{p,q} &= cov\left(x_p(t), x_q(t)\right) \\ &= E\left[\left(x_p(t) - \mu_p\right)\left(x_q(t) - \mu_q\right)^H\right] \\ &= \frac{1}{T}\sum_{k=1}^{T}\left(x_{p.k}(t) - \mu_p\right)\left(x_{q.k}(t) - \mu_q\right)^* \end{aligned} \tag{2.5}$$

where $(.)^*$ is conjugate, μ_p and μ_q are the statistical means associated with $x_{p.k}(t)x_{q.k}(t)$ respectively. Here, $x_{p.k}(t)$ and $x_{q.k}(t)$ represent complex-valued data and by expressing it in complex form, Equation (2.5) can be expressed as

$$\begin{aligned} r_{p,q} = \frac{1}{T}\sum_{k=1}^{T} &\left(\Re(x_{p.k}(t)) + j(\Im(x_{p.k}(t))) - \Re(\mu_p)\right. \\ &\left. - j(\Im(\mu_p))\right)\left(\Re(x_{q.k}(t)) + j(\Im(x_{q.k}(t))) - \Re(\mu_q) - j(\Im(\mu_q))\right)^* \end{aligned} \tag{2.6}$$

where $\Re(.)$ and $\Im(.)$ are the real and imaginary part of (.) respectively.

Upon further simplification of Equation (2.6), it follows

$$\begin{aligned} r_{p,q} = &cov(\Re(x_{p.k}(t), \Re\left(x_{q.k}(t)\right)) + cov(\Im(x_{p.k}(t), \Im(x_{q.k}(t)) \\ &- j\left(cov(\Re(x_{p.k}(t), \Im\left(x_{q.k}(t)\right)\right) - cov(\Im(x_{p.k}(t), \Re\left(x_{q.k}(t)\right))\right) \end{aligned} \tag{2.7}$$

Finally, by considering the covariance property for complex-valued signals, $r_{p,q}$ can be expressed as

$$r_{p,q} = cov\left(x_p(t), x_q(t)\right) = \left(\frac{1}{T}\sum_{k=1}^{T}\left|x_{p.k}(t)\right|\right)\left(\frac{1}{T}\sum_{k=1}^{T}\left|x_{q.k}(t)\right|\right)e^{j\Delta\phi} \tag{2.8}$$

where $|.|$ represents the magnitude of $(.)$ and $\Delta\phi$ is the phase difference between $x_{p.k}(t)$ and $x_{q.k}(t)$ and it is given by

$$\Delta\phi = \left(\frac{1}{T}\sum_{k=1}^{T}\arg\left(x_{p.k}(t)\right)\right) - \left(\frac{1}{T}\sum_{k=1}^{T}\arg\left(x_{q.k}(t)\right)\right) \tag{2.9}$$

where arg is the *arctan* function.

From Equation (2.8), $r_{p,q}$ contains both the in-phase and quadrature information of the phase difference. Additionally, $r_{p,q}$ is normalized to remove the magnitude information of the $x_{p.k}(t)$ and $x_{q.k}(t)$, resulting in

$$u_{p,q} = \frac{r_{p,q}}{\|r_{p,q}\|} = e^{j\Delta\phi} = \cos\left(\Delta\phi\right) + j\sin(\Delta\phi) \tag{2.10}$$

where $\|.\|$ denotes the norm of $(.)$. The strength of the correlation in the quadrature (imaginary) direction between $x_{p.k}(t)$ and $x_{q.k}(t)$ guarantee the uniqueness of mapping. Therefore, the $\Im\left(u_{p,q}\right)$ is considered as an input feature to train ML models as observed in Fig. 2.1. Here, $\Im\left(u_{p,q}\right) = 0$ for $p = q$, therefore the principal diagonal elements of $\widehat{\mathbf{R}}$ are not included in the feature vector. Thus, the feature vector for training the ML model is given by

$$\boldsymbol{v} = [v_{1,2}, v_{1,3}, \ldots, v_{1,N}, v_{2,3}, \ldots, v_{2,N}, \ldots, v_{N,N-1}] \in \mathbb{R}^{1\times N(N+1)} \tag{2.11}$$

where $v_{p,q} = \Im\left(u_{p,q}\right)$.

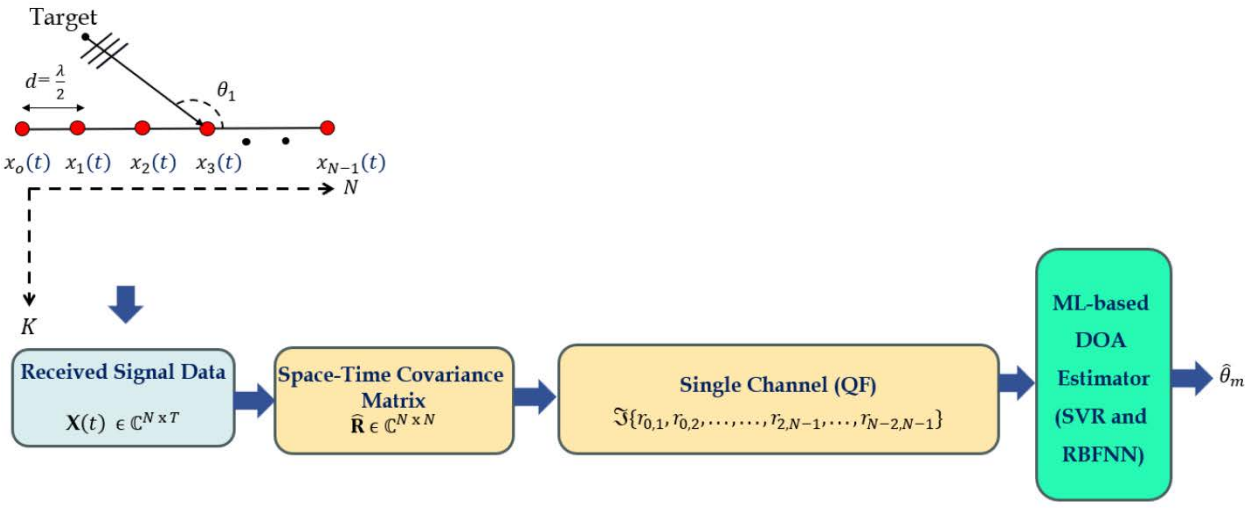

Figure 2.1: Process flow of the single channel approach

2.1.1 Training Setup

The training phase is an offline process in which the DoA estimation model $\widehat{F}\colon \boldsymbol{v} \rightarrow \theta$ is obtained from the available training pairs through the process of learning with ML models. For simplicity, the training process is explained for $M = 1$. The generated set of L training pairs used for learning is given by $\{\boldsymbol{v}_1, \theta_1), (\boldsymbol{v}_2, \theta_2), \ldots, (\boldsymbol{v}_l, \theta_l), \ldots, (\boldsymbol{v}_L, \theta_L)\}$. To acquire the training set, the array STCM $\widehat{\mathbf{R}}^l$ is computed for each angle θ_l, which is uniformly distributed in the range. -90° to$+90^\circ$ i.e., $\theta_l = -90^\circ + (l-1)\,\Delta\theta, l = 1, 2, \ldots L$, where $\Delta\theta$ is the angular separation. Then, the feature vector $\boldsymbol{v}_l$ for each angle θ_l is computed from the corresponding STCM $\widehat{\mathbf{R}}^l$ using Equation (2.11). Note that the DoA estimation model $\widehat{F}\colon \boldsymbol{v} \rightarrow \theta$ can be obtained by using any ML models such as RBFNN and SVR, for the given training pairs through proper tuning of hyperparameters [11, 21]. The brief description of RBFNN and SVR models is as follows.

2.1.2 Testing Setup

In the testing (estimation) phase, the trained DoA estimation models $\widehat{F}_{RBFNN}(\boldsymbol{v})$ and $\widehat{F}_{SVR}(\boldsymbol{v})$ are utilized to estimate the unknown M DoA's $\{\theta_m\}_{m=1}^{M}$ of the incoming targets. These estimates are computed as

$$\{\hat{\theta}_{m=1}^{M}\} = \widehat{F}(\boldsymbol{v}^m) \tag{2.12}$$

where $\boldsymbol{v}^m$ represents the feature vector of m^{th} target and it is computed from the array STCM $\widehat{\mathbf{R}}$ using Equation (2.11).

2.2 Simulation Results and Analysis

2.2.1 Complexity Analysis

The assessment of complexity is conducted in terms of the number of complex multiplications involved in both the training and testing phases. In both phases, the complexities depend on two computations: the computation of the STCM and the model complexity. The training and testing complexities of the proposed approach are compared with those of the existing approach, as summarized in Table 2.1 and 2.2. It is evident that the proposed approach

	Method	Complexity
Existing Approach	RBFNN [10–13]	Training Complexity $O\left(N^2T + CLN(N+1)\right)$
		Testing Complexity $O\left(N^2T + CN(N+1)\right)$
	SVR [14, 15]	Training Complexity $O\left(N^2T + L^2N(N+1)\right)$
		Testing Complexity $O\left(N^2T + n_{sv}N(N+1)\right)$

Table 2.1: Complexity comparison (Existing approach)

	Method	Complexity
Proposed Approach	RBFNN	Training Complexity $O\left(N^2T + CL\left(\left(\frac{N(N+1)}{2}\right) - N\right)\right)$
		Testing Complexity $O\left(N^2T + C\left(\left(\frac{N(N+1)}{2}\right) - N\right)\right)$
	SVR	Training Complexity $O\left(N^2T + L^2\left(\left(\frac{N(N+1)}{2}\right) - N\right)\right)$
		Testing Complexity $O\left(N^2T + n_{sv}\left(\left(\frac{N(N+1)}{2}\right) - N\right)\right)$

Table 2.2: Complexity comparison (Proposed approach)

involves less computational complexity compared to the existing approach where $O(N^2T)$ is the STCM complexity, and the remaining one is the model complexity of RBFNN and SVR during the training and testing phases respectively. Here, N is the number of array elements, T is the number of data snapshots, L is the number of training samples, C is the number of centers in RBFNN and n_{sv} is the number of support vectors in SVR.

2.2.2 Estimation Reliability

In this experiment, the estimation reliability of the proposed approach is assessed under two conditions: with no noise ($\sigma_n^2 = 0$) and with noise ($\sigma_n^2 = 0.1$, corresponding to an SNR of 10 dB), considering $M = 1$, $N = 5$ and $T = 1000$. For the training phase, randomly generated $L = 162$ samples ranging from $-90°$ to $+90°$ with a step size of $\Delta\theta = 1°$ are used to train the model. Additionally, $L = 19$ samples are reserved for the testing phase, which is not included in the training phase. The hyperparameters of RBFNN and SVR model during the training phase are chosen as follows: for existing: $C = 100$ (number of centers), $\sigma = 0.1$(width of RBFNN function), $\zeta = 100$ (regularization constant in SVR), $\varepsilon = 1$ (error limit in SVR) and $\gamma = 0.5$ (kernel parameter). For the proposed: $C = 100$, $\sigma = 1$, $\zeta = 100, \varepsilon = 1$ and $\gamma = 0.5$ The selection of hyperparameter values based on the training phase accuracy for different sets of hyperparameters are presented in Appendix A.1 The results, as depicted in Fig. 2.2 (a)-(h), show that the proposed approach consistently estimates true DoAs with higher accuracy compared to the existing approach for both ML models under both noise conditions.

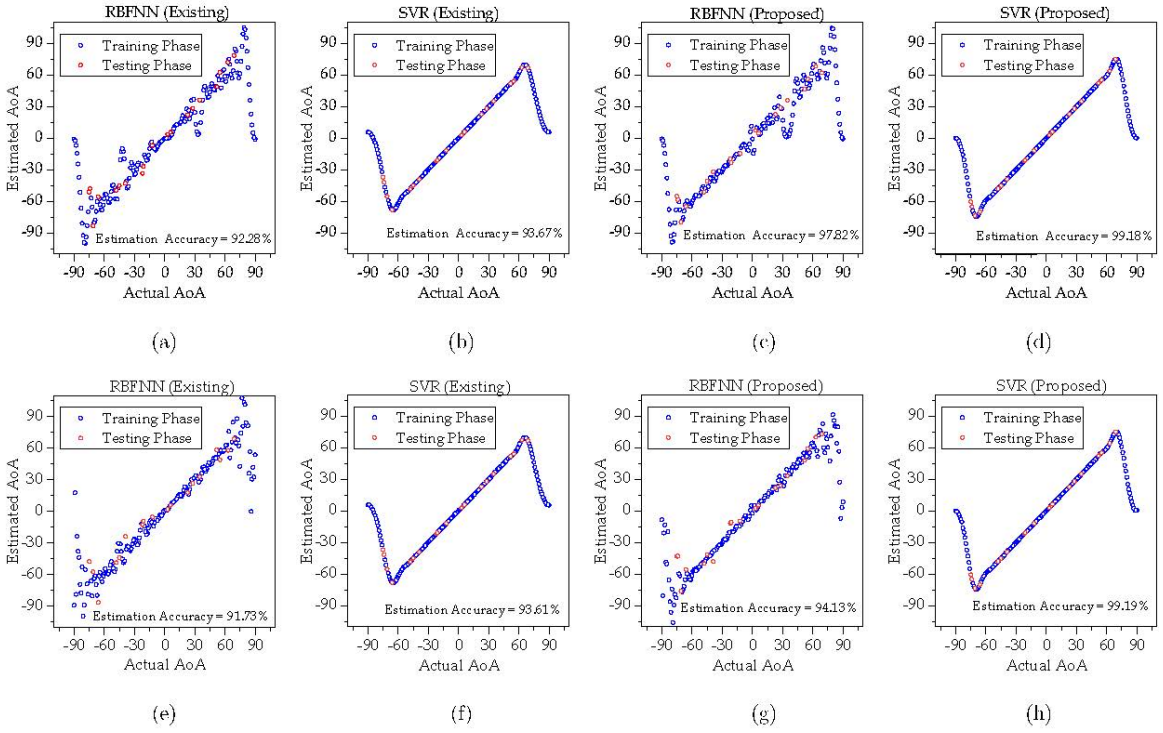

Figure 2.2: Reliability comparison: (a)-(d) under $\sigma_n^2 = 0$, (e)-(h) under $\sigma_n^2 = 0.1$

2.2.3 Estimation Accuracy

In this experiment, the estimation accuracy is assessed for different variations of the number of array elements, number of snapshots and SNR. For the evaluation of estimation accuracy as a function of the number of array elements variations i.e., $2 \leq N \leq 15$ for a fixed $T = 1000$ and $\sigma_n^2 = 0.1$(SNR of 10 dB). From Fig. 2.3, it is evident that the proposed SVR approach achieves superior accuracy over the existing SVR approach, even with a low number of array elements. Additionally, the proposed RBFNN approach consistently outperforms the existing RBFNN approach as the number of elements increases. For the evaluation of the estimation accuracy as a function of snapshot variations i.e., $10 \leq T \leq 500$ for a fixed $N = 5$ and $\sigma_n^2 = 0.1$(SNR of 10 dB). From Fig. 2.4, it is evident that the proposed SVR approach exhibits superior estimation performance compared to the existing approaches. Additionally,

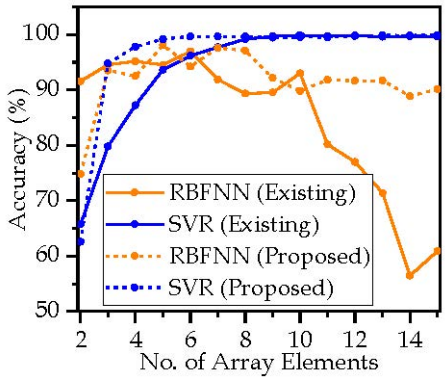

Figure 2.3: Accuracy comparison versus number of array elements

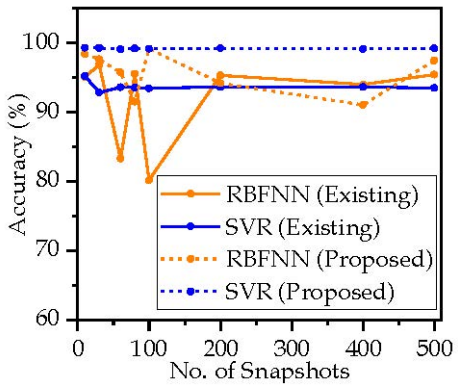

Figure 2.4: Accuracy comparison versus number of snapshots

the proposed RBFNN approach maintains consistency and outperforms the existing RBFNN approach as the number of snapshots increases. Lastly, the estimation accuracy is evaluated for different SNR variations i.e., $-20\text{dB} \leq \text{SNR} \leq +20\text{dB}$ for a fixed $N = 5$ and $T = 1000$. From Fig. 2.5, it is clear that the proposed SVR approach consistently exhibits superior estimation accuracy compared to the existing approaches, even at low SNR regimes.

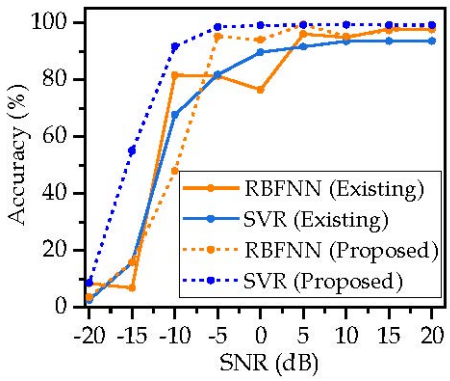

Figure 2.5: Accuracy comparison versus SNR

2.2.4 Computation Complexity and Execution Time

The training and testing computation complexity is evaluated for different variations in the number of array elements i.e., $3 \leq N \leq 10$ with fixed $T = 1000, C = 100$, $L = 162$ and n_{sv}. From Fig. 2.6 and Fig. 2.7, it is evident that the proposed SVR approach effectively reduces the computational complexity by about half compared to the existing SVR approach

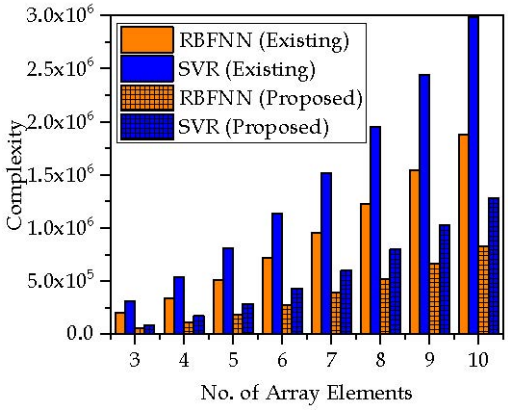

Figure 2.6: Training complexity comparison versus number of array elements

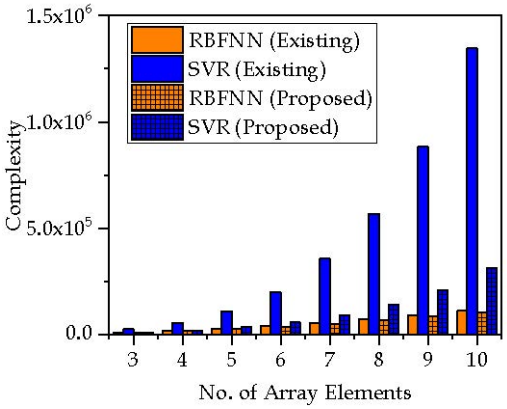

Figure 2.7: Testing complexity comparison versus number of array elements

Approaches	RBFNN	SVR
Existing	0.00152 seconds	0.00802 seconds
Proposed	0.00101 seconds	0.00171 seconds

Table 2.3: Execution time comparison

for all variations of N. Furthermore, the proposed RBFNN approach demonstrates the lowest computational complexity in the training phase but does not exhibit significant reduction compared to the existing approach in the testing phase, attributed to its small training samples. The execution time is measured with $N = 5, T = 1000$, on a PC equipped with a 1.8GHz processor and 8GB of RAM. From Table 2.3, the findings reveal that the proposed approach (testing phase) exhibits notable speed improvements, demonstrating significantly reduced time requirements.

Chapter 3

Modified Single Channel Approach

This section details the formulation of the modified single channel approach. Simulation results of the proposed approach and the existing approach are compared across various metrics such as estimation reliability, accuracy, and execution time.

3.1 Proposed Formulation

The modified proposed approach aims to approximate the unknown mapping that relates the phase of the array of the STCM ($\measuredangle(\mathbf{R})$) to its corresponding DoA (θ) of the incoming targets. From Equation (2.10), the phase ($\measuredangle$) is computed for $u_{p,q}$ which is obtained by normalizing $r_{p,q}$. It is expressed as

$$\measuredangle(u_{p,q}) = \tan^{-1}(\cos(\Delta\varphi) + jsin(\Delta\varphi)) \tag{3.1}$$

The equation results in

$$\measuredangle(u_{p,q}) = \tan^{-1}\left(\frac{sin(\Delta\varphi)}{\cos(\Delta\varphi)}\right) \tag{3.2}$$

$$\measuredangle(u_{p,q}) = \Delta\varphi \tag{3.3}$$

The uniqueness of mapping is guaranteed as depicted in Fig. 3.1 for the setup of $N = 5$ and $T = 1000$. Hence, we can use $(u_{p,q})$ as the feature vector to the ML models and expect more accurate predictions as compared to the existing approach.

The pre-processing steps involved to generate the feature vectors in the modified single channel approach is depicted in Fig. 3.2. This process helps map each θ from $-90°$ to $+90°$

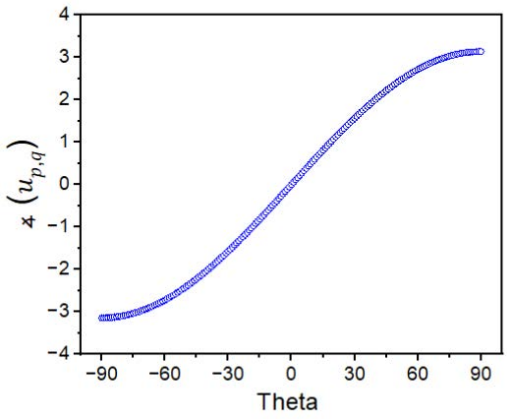

Figure 3.1: $\measuredangle(u_{p,q})$ versus theta

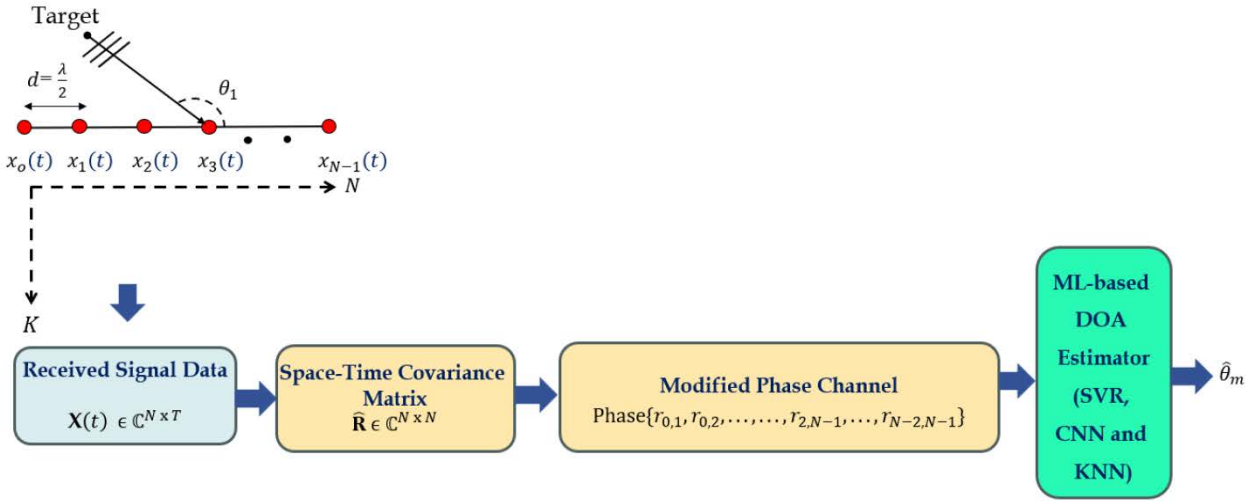

Figure 3.2: Process flow of the modified single channel approach

to its corresponding feature vector. This information is then used in the training and testing stages that is ultimately fed into the machine learning models for prediction.

3.2 Simulation Results and Analysis

3.2.1 Estimation Reliability

In this experiment, the estimation reliability of the proposed approach is assessed using KNN, CNN and SVR under two conditions: with no noise ($\sigma_n^2 = 0$) and with noise ($\sigma_n^2 = 0.1$,

corresponding to an SNR of 10dB), considering $M = 1$, $N = 5$ and $T = 1000$. For the training phase, all samples ranging from $-90°$ to $+90°$ with a step size of $\Delta\theta = 1°$ are used to train the model. Additionally, $L = 9$ samples from the enfires are reserved for the testing phase. The hyperparameters for KNN, CNN and SVR are chosen as follows: for existing: *number of neighbours* $= 2$ in KNN [28]; 3 convolutional layers with kernels of size 3×3, 1 pooling layer, 3 fully connected layers in CNN [26, 27] and $\zeta = 100$, $\varepsilon = 1$ and $\gamma = 0.5$ in SVR [14, 15]. For the proposed: *number of neighbours* $= 1$ in KNN; 3 convolutional layers with kernels of size 3×3, 1 pooling layer, 3 fully connected layers in CNN and $\zeta = 100$, $\varepsilon = 0.4$ and $\gamma = 0.5$ in SVR. The selection of hyperparameter values based on the training phase accuracy for different sets of hyperparameters is presented in Appendix A.2 The results, as depicted in Fig. 3.3 (a)-(f) and Fig. 3.3 (g)-(l), show that the proposed approach consistently estimates true DoAs with higher accuracy compared to the existing approach for both ML models under both noise conditions.

3.2.2 Estimation Accuracy

In this experiment, the estimation accuracy is assessed for different variations of the number of array elements, number of snapshots and SNR. Additionally, the estimation accuracy is evaluated with $\Delta\theta = 5°$ and under the influence of mutual coupling. For the evaluation of estimation accuracy as a function, the models are trained with $T = 1000$ and noise-free condition and tested with varied number of array elements i.e., $2 \leq N \leq 10$ for a fixed $T = 100$ and $\sigma_n^2 = 0.1$(SNR of 10dB). From Fig. 3.4, it is evident that the proposed SVR and CNN approach achieves superior accuracy over the existing SVR and CNN approach, even with a low number of array elements. Additionally, the proposed KNN approach not only consistently outperforms the existing KNN approach but also is the best overall model as the number of elements increases. For the evaluation of the estimation accuracy as a function, the models are trained with $N = 5$ and noise-free condition and tested with varied number of snapshots i.e., $10 \leq T \leq 1000$ for a fixed $N = 5$ and $\sigma_n^2 = 0.1$(SNR of 10dB). From Fig. 3.5, it is evident that the proposed KNN approach exhibits superior estimation performance compared to the existing approaches. Additionally, the proposed SVR and CNN approach maintains consistency and outperforms the existing SVR and CNN approach as the number of snapshots

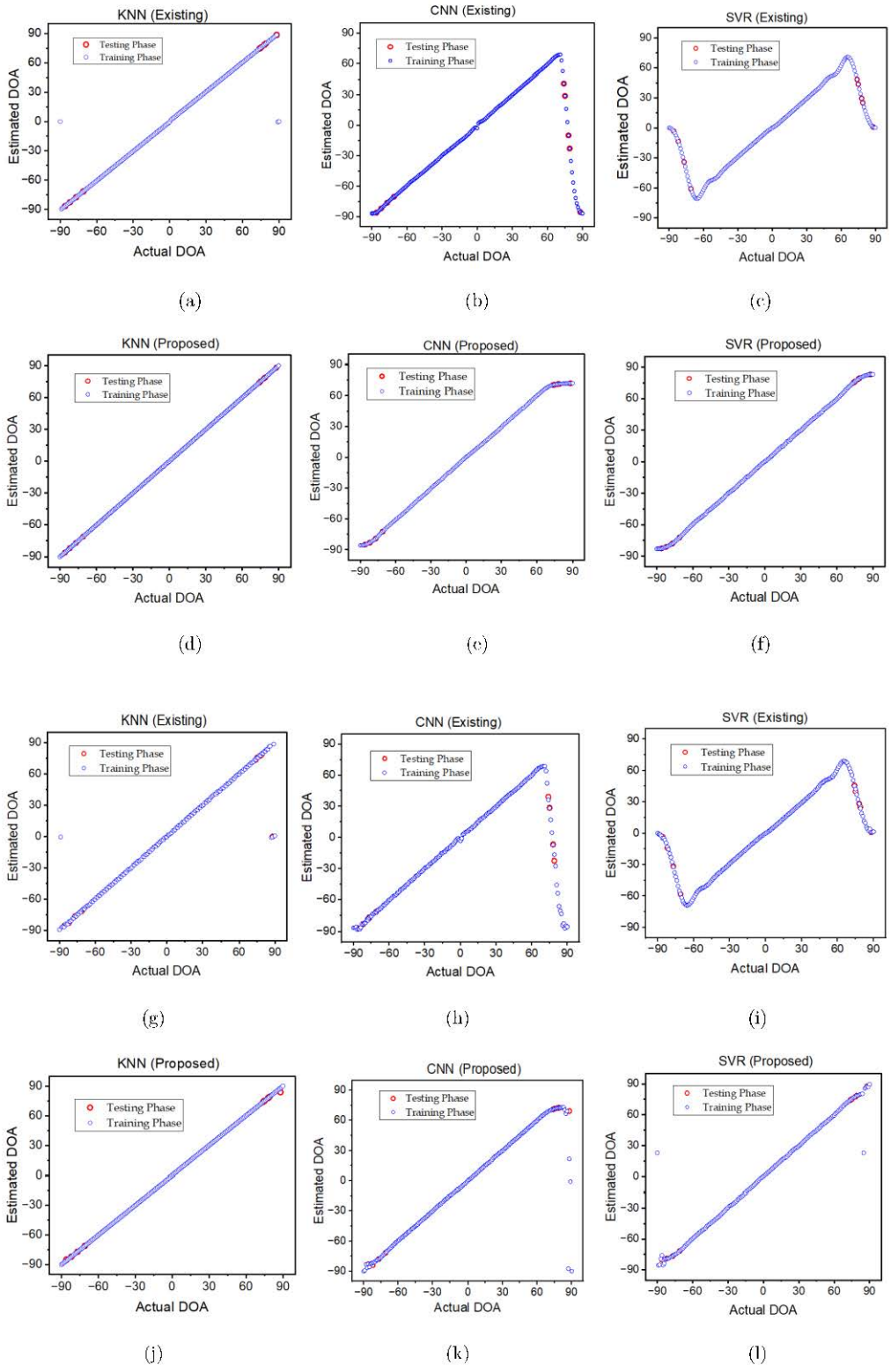

Figure 3.3: Reliability of endfire prediction comparison: (a)-(f) under $\sigma_n^2 = 0$, (g)-(l) under $\sigma_n^2 = 0.1$

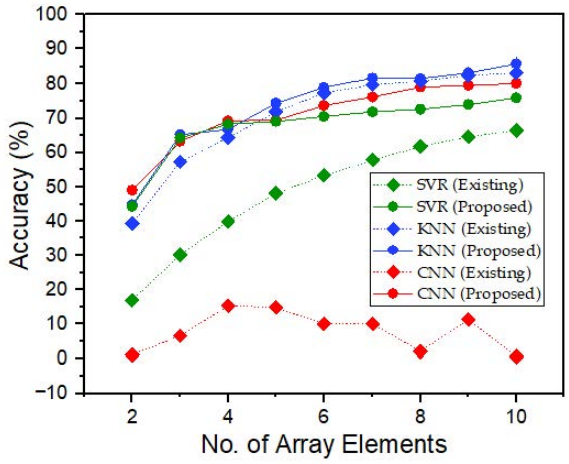

Figure 3.4: Accuracy of endfire prediction versus number of array elements

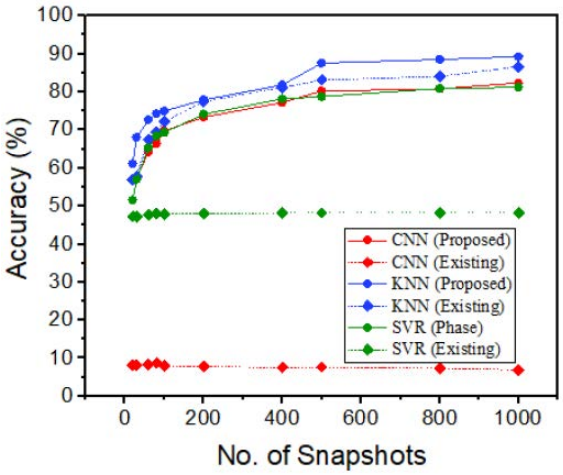

Figure 3.5: Accuracy of endfire prediction versus number of snapshots

increases. Lastly, the estimation accuracy is evaluated for different SNR variations, where the models are trained with $N = 5$, $T = 1000$ and under no noise and tested with varied noise i.e., $-20\text{dB} \leq \text{SNR} \leq +20\text{dB}$ for a fixed $N = 5$ and $T = 100$. From Fig. 3.6, it is clear that the proposed KNN approach consistently exhibits superior estimation accuracy compared to the existing approaches, even at low SNR regimes.

For the evaluation of accuracy in Table 3.1, the models are trained with $N = 7$, $T = 1000$ and $\Delta\theta = 5^\circ$ ranging from $-90^\circ$to $+90^\circ$ and tested with $L = 9$ samples for a setup of $N = 7$,

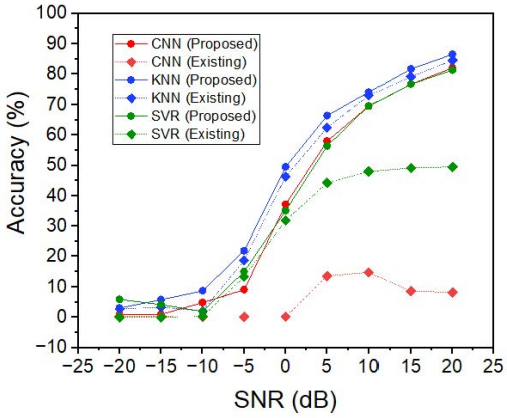

Figure 3.6: Accuracy of endfire prediction versus SNR

Approach	Model	Training Accuracy	Testing Accuracy
Proposed	KNN	99.99%	96.12%
	CNN	99.17%	94.20%
	SVR	99.81%	90.47%
Existing	KNN	77.18%	81.26%
	CNN	21.50%	1.61%
	SVR	65.54%	53.51%

Table 3.1: Training and testing accuracy comparison for $\Delta\theta = 5°$

$T = 1000$ and $\sigma_n^2 = 0.1$(SNR of 10dB). We can observe that all the proposed models have better training and testing accuracies as compared to the existing models. Notably, it can be inferred that the proposed KNN approach has the best estimation even when trained with a smaller number of samples and tested under harsh conditions.

In Fig. 3.7, we compare accuracy with the influence of mutual coupling. It is the unexpected increase in noise due to the interaction between array elements when spaced close to each other [24, 25]. Mutual coupling is computed as follows

$$C_1 = 0.65e^{j\left(\frac{\pi}{7}\right)} \tag{3.4}$$

$$C_2 = 0.25e^{j\left(\frac{\pi}{10}\right)} \tag{3.5}$$

$$\mathbf{M}(t) = \begin{pmatrix} 1 & C_1 & C_2 & 0 & \cdots & 0 \\ C_1 & 1 & C_1 & C_2 & 0 & 0 \\ C_2 & C_1 & 1 & C_1 & C_2 & 0 \\ 0 & C_2 & C_1 & 1 & C_1 & 0 \\ \vdots & 0 & C_2 & C_1 & \ddots & \vdots \\ 0 & 0 & 0 & 0 & \cdots & 1 \end{pmatrix}_{N \times N} \tag{3.6}$$

where $C_1 \geq C_2$. $\mathbf{M}(t)$ is included while computing the data model as

$$\mathbf{x}(t) = \mathbf{M}(t)\mathbf{A}(t)s(t) + \mathbf{n}(t) \tag{3.7}$$

The machine learning models are trained with C_1 and C_2 as shown in Equation (18) and (19) and tested with varied values of C_1. The training setup is $N = 7$ and $T = 1000$ under noise-free condition and testing setup is $N = 10$ and $T = 500$ under $\sigma_n^2 = 0.1$(SNR of 10dB). As observed in Fig. 3.7, the proposed approach models showcase better accuracy when compared to the existing approach models especially, in CNN.

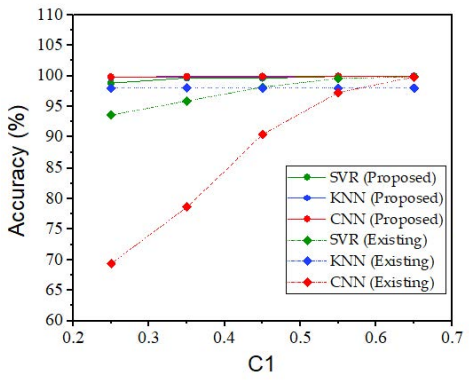

Figure 3.7: Accuracy versus C_1

3.2.3 Execution time

The execution time is measured with $N = 10, T = 1000$ and $\sigma_n^2 = 0.1$ (10dB SNR) on a PC equipped with a 1.8GHz processor and 8GB of RAM. From Table 3.2, the findings reveal that all the proposed approaches (testing phase) exhibit notable speed improvements,

Model	Proposed Approach	Existing Approach
KNN	0.05278 seconds	0.05974 seconds
CNN	0.10915 seconds	0.11157 seconds
SVR	0.00238 seconds	0.01044 seconds

Table 3.2: Execution time comparison (Modified Single Channel Approach)

demonstrating significantly reduced time requirements. The proposed SVR, specifically, displays significant reduction in execution time as compared to the existing SVR approach.

Chapter 4

Conclusion and Future Perspectives

In this thesis, the challenge of ML- based DoA estimation is tackled by introducing two novel approaches. The single channel approach demonstrates better estimation reliability; estimation accuracy under conditions of fewer array elements, reduced snapshots and low SNR. Additionally, it reduces the computational complexity and execution time drastically when compared to the existing approach. However, since the issue of endifre prediction isn't tackled, a modified singled channel approach is proposed. It demonstrates better estimation reliability and accuracy for endfire prediction under conditions such as varied number of array elements, number of snapshots, SNR values and mutual coupling. Moreover, it showcases better estimation reliability when trained with a step size of $\Delta\theta = 5^\circ$ and exhibits quicker execution time when compared with the existing approach.

The proposed approach can further be verified using various other ML techniques like bagging and boosting, which haven't been employed conventionally. Furthermore, the challenge of SIMO (Single Input Multiple Output) DoA estimation using ML needs to be addressed.

Appendix A

In Appendix A, simulation analysis for the selection of hyperparameter values based on the training phase accuracy for different sets of hyperparameters is presented in Fig. A.1 and Fig. A.2, considering $M = 1$, $N = 5$ and $T = 1000$ under $\sigma_n^2 = 0$.

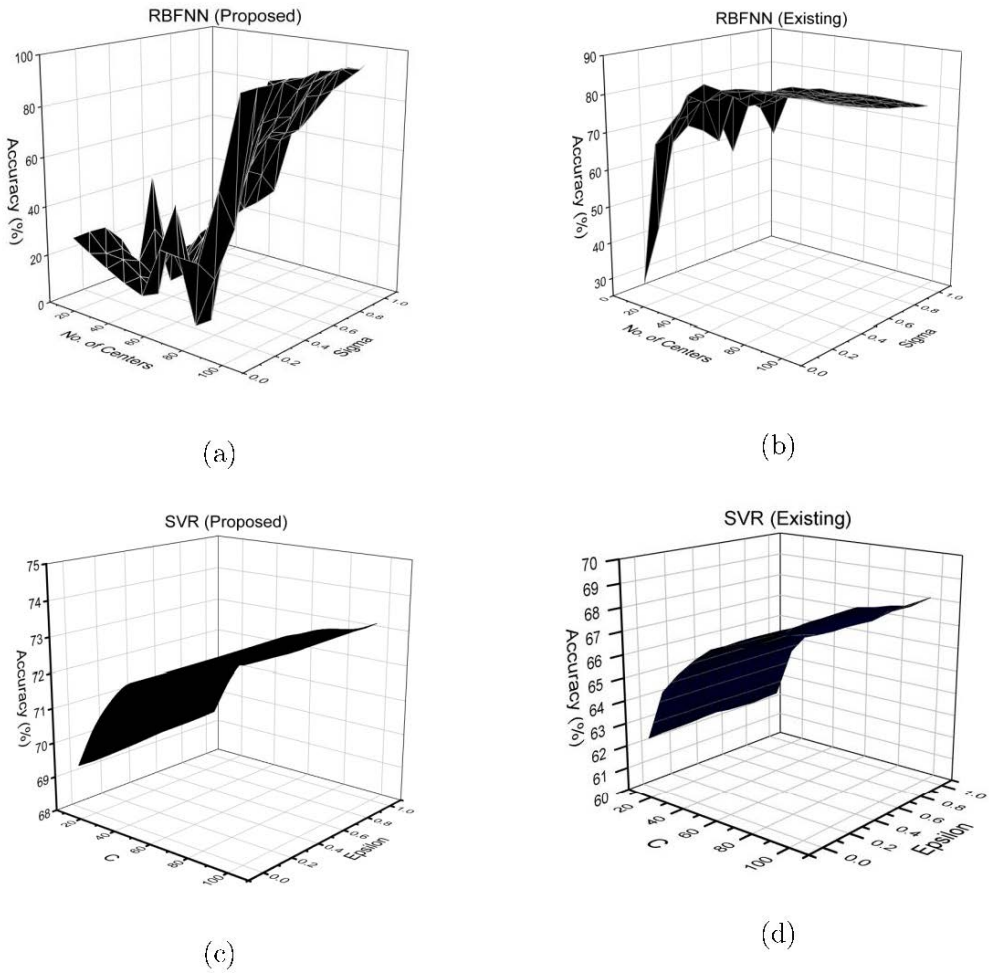

Figure A.1: Training accuracy versus hyperparameters (Single Channel Approach)

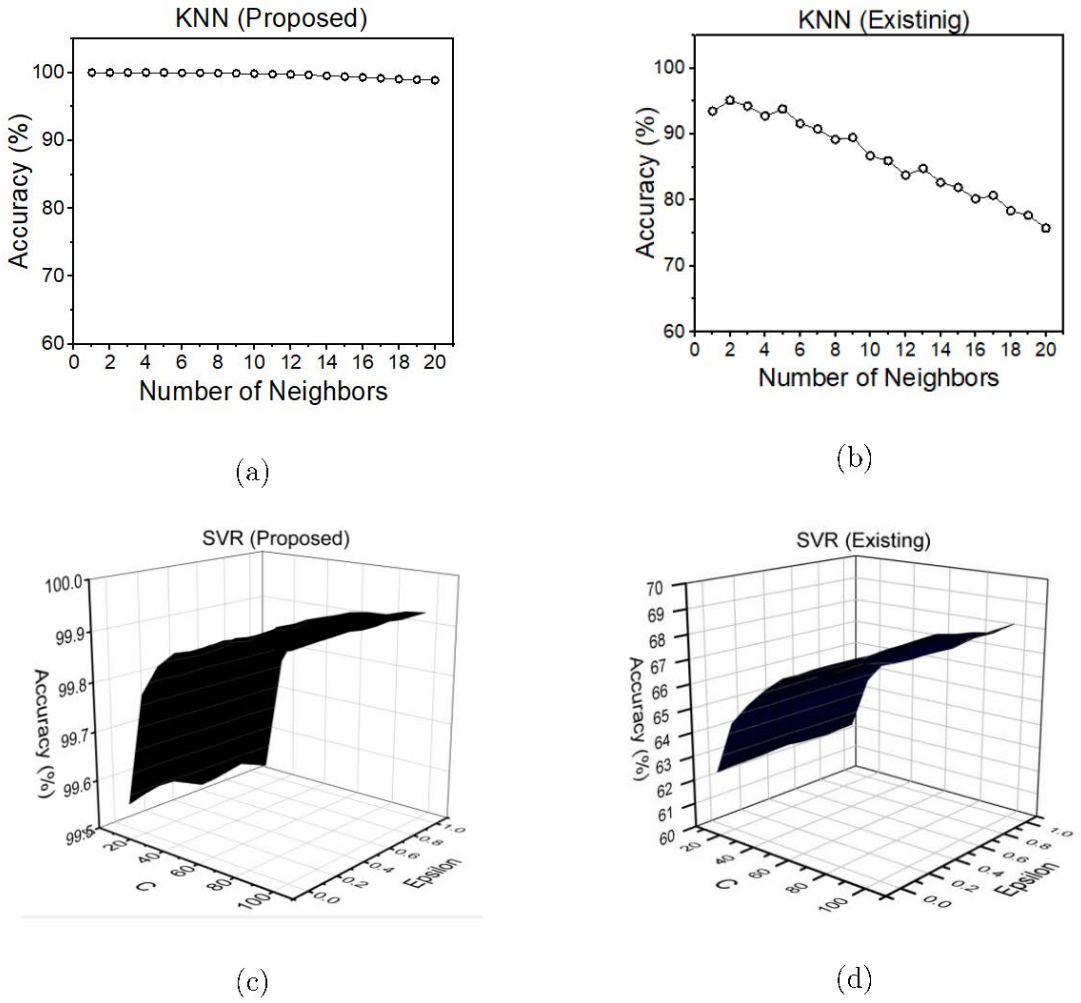

Figure A.2: Training accuracy versus hyperparameters (Modified Single Channel Approach)

Publications

1. Ashok Chandrasekaran and **Ishaan Reddy**, "An Efficient Approach for Machine Learning-based Angle-of-Arrival Estimation", Applied Soft Computing, 2024. *(Under Review)*

2. Ashok Chandrasekaran and **Ishaan Reddy**, "Improved DOA Estimation at Array Endfire using modified Machine Learning approach", IEEE Transactions on Machine Learning in Communications and Networking. *(Under Preparation)*

3. **Ishaan Reddy** and Ashok Chandrasekaran, "An Efficient Approach for Machine Learning-based Direction-of-Arrival Estimation of Targets in Passive RADAR", Peeref 5-min Research Presentation Challenge 2024.
   https://doi.org/10.54985/peeref.2401w7871726

References

[1] H. Krim and M. Viberg, "Two decades of array signal processing research: the parametric approach," in *IEEE Signal Processing Magazine*, vol. 13, no. 4, pp. 67–94, July 1996.

[2] M. Pesavento, M. Trinh-Hoang and M. Viberg, "Three More Decades in Array Signal Processing Research: An optimization and structure exploitation perspective," in *IEEE Signal Processing Magazine*, vol. 40, no. 4, pp. 92–106, June 2023.

[3] W. Liu, M. Haardt, M. S. Greco, C. F. Mecklenbräuker and P. Willett, "Twenty-Five Years of Sensor Array and Multichannel Signal Processing: A review of progress to date and potential research directions," in *IEEE Signal Processing Magazine*, vol. 40, no. 4, pp. 80–91, June 2023.

[4] T. E. Tuncer and B. Friedlander, Classical and Modern Direction-of- Arrival Estimation. New York, NY, USA: Academic, 2009.

[5] R. Schmidt, "Multiple emitter location and signal parameter estimation," in *IEEE Trans. Antennas Propag.*, vol. AP-34, no. 3, pp. 276–280, Mar. 1986.

[6] R. Roy and T. Kailath, "ESPRIT-estimation of signal parameters via rotational invariance techniques," in *IEEE Trans. Acoust., Speech, Signal Process.*, vol. 37, no. 7, pp. 984–995, Jul. 1989.

[7] Q. Shen, W. Liu, W. Cui and S. Wu, "Underdetermined DOA Estimation Under the Compressive Sensing Framework: A Review," in *IEEE Access*, vol. 4, pp. 8865–8878, 2016.

[8] Z. Yang, J. Li, P. Stoica and L. H. Xie, "Sparse methods for direction-of-arrival estimation" in Array Radar and Communications Engineering, New York, NY, USA: Academic, pp. 509–581, 2018.

[9] Ming-Yi You, An-Nan Lu, Yun-Xia Ye, Kai Huang, Bin Jiang, "A Review on Machine Learning-Based Radio Direction Finding," in *Mathematical Problems in Engineering*, (9), 2020.

[10] Y. Zheng, Y. Xiao, Z. Ma, P. D. Diamantoulakis and G. K. Karagiannidis, "Neural Network-Based Multi-DOA Tracking for High Speed Railway Communication Systems," in *IEEE Transactions on Vehicular Technology*, vol. 71, no. 10, pp. 11284–11288, Oct. 2022.

[11] Y. Guo, Z. Zhang, Y. Huang and P. Zhang, "DOA Estimation Method Based on Cascaded Neural Network for Two Closely Spaced Sources," in *IEEE Signal Processing Letters*, vol. 27, pp. 570–574, 2020.

[12] A. H. El Zooghby, C. G. Christodoulou and M. Georgiopoulos, "A neural network-based smart antenna for multiple source tracking," in *IEEE Transactions on Antennas and Propagation*, vol. 48, no. 5, pp. 768–776, May 2000.

[13] A. H. El Zooghby, C. G. Christodoulou and M. Georgiopoulos, "Performance of radial-basis function networks for direction of arrival estimation with antenna arrays," in *IEEE Transactions on Antennas and Propagation*, vol. 45, no. 11, pp. 1611–1617, Nov. 1997.

[14] L. -L. Wu and Z. -T. Huang, "Coherent SVR Learning for Wideband Direction-of-Arrival Estimation," in *IEEE Signal Processing Letters*, vol. 26, no. 4, pp. 642–646, April 2019.

[15] A. Randazzo, M. A. Abou-Khousa, M. Pastorino and R. Zoughi, "Direction of arrival estimation based on support vector regression: Experimental validation and comparison with music," in *IEEE Antennas Wireless Propag. Lett.*, vol. 6, no. 11, pp. 379–382, 2007.

[16] Ashok. C and Venkateswaran. N, "Manifold Ambiguity-Free Low Complexity DOA Estimation Method for Unfolded Co-Prime Arrays," in *IEEE Communications Letters*, vol. 25, no. 6, pp. 1886–1890, June 2021.

[17] Ashok, C., Venkateswaran, N, "An Efficient Method for Resolving Ambiguity in DOA Estimation with Coprime Linear Array," in *Circuits Syst. Signal Process*, vol. 41, pp. 2411–2427, 2022.

[18] S. Scardapane, S. Van Vaerenbergh, A. Hussain and A. Uncini, "Complex-Valued Neural Networks With Nonparametric Activation Functions," in *IEEE Transactions on Emerging Topics in Computational Intelligence*, vol. 4, no. 2, pp. 140–150, April 2020.

[19] T. Adali, P. J. Schreier and L. L. Scharf, "Complex-Valued Signal Processing: The Proper Way to Deal With Impropriety," in *IEEE Transactions on Signal Processing*, vol. 59, no. 11, pp. 5101–5125, Nov. 2011.

[20] N. Soleimani and R. Trinchero, "Compressed complex-valued least squares support vector machine regression for modeling of the frequency-domain responses of electromagnetic structures," Electronics, vol. 11, no. 4, p. 551, Feb. 2022.

[21] V. Cherkassky and Y. Ma, "Practical selection of SVM parameters and noise estimation for SVM regression," in *Neural Netw.*, vol. 17, no. 1, pp. 113–126, Jan. 2004.

[22] A. J. Smola and B. Schölkopf, "A tutorial on support vector regression," *Statist. Comput.*, vol. 14, no. 3, pp. 199–222, Aug. 2004.

[23] V. Vapnik, S. Golowich, and A. J. Smola, "Support vector method for function approximation, regression estimation, and signal processing," in *Neural Information Processing Systems*, vol. 9. Cambridge, MA, USA: MIT Press, 1997.

[24] C. S. Ateavcı, Y. Bahadırlar and S. Aldırmaz-Çolak, "DoA Estimation in the Presence of Mutual Coupling Using Root-MUSIC Algorithm," *2021 8th International Conference on Electrical and Electronics Engineering (ICEEE)*, Antalya, Turkey, 2021, pp. 292–298.

[25] J. Kota, A. Madanayake, L. Belostotski, C. Wijenayake and L. T. Bruton, "A 2-D Signal Processing Model to Predict the Effect of Mutual Coupling on Array Factor," in *IEEE Antennas and Wireless Propagation Letters*, vol. 12, pp. 1264–1267, 2013.

[26] Zhao F, Hu G, Zhan C, Zhang Y. DOA Estimation Method Based on Improved Deep Convolutional Neural Network. Sensors. 2022; 22(4):1305.

[27] Yuji Liu, Huixiu Chen, Biao Wang, DOA estimation based on CNN for underwater acoustic array, Applied Acoustics, Volume 172, 2021.

[28] Y. Liu, H. Chen and B. Wang, "DOA Estimation of Underwater Acoustic Signals Based on PCA-kNN Algorithm," 2020 International Conference on Computer Information and Big Data Applications (CIBDA), Guiyang, China, 2020, pp. 486–490.